J. Membrane Biol. 153, 217–231 (1996)

The Journal of
Membrane
Biology

A Ca^{2+} Current Activated by Release of Intracellular Ca^{2+} Stores in Rat Basophilic Leukemia Cells (RBL-1)

G.G. Schofield, M.J. Mason
Department of Physiology, Tulane University Medical School, 1430 Tulane Avenue, New Orleans, Louisiana 70112

Received: 12 September 1995/Revised: 18 June 1996

Abstract. We have characterized a Ca^{2+} current activated by depletion of intracellular Ca^{2+} stores (capacitative Ca^{2+} entry current) as a first step to investigate the mechanisms underlying communication between the intracellular Ca^{2+} stores and the plasma membrane Ca^{2+} permeability. Whole cell currents in response to voltage ramps from −125 to +60 mV from a holding potential of −40 mV were recorded in rat basophilic leukemia cells (RBL-1 cells) in solutions designed to optimize detection of a Ca^{2+} current. An inwardly rectifying current could be activated upon dialysis of the cell interior with pipette solutions devoid of Ca^{2+} and containing 20 mM BAPTA, a procedure expected to passively deplete intracellular Ca^{2+} stores. The current was maximally activated within 2 min, was sensitive to extracellular Ca^{2+} concentration and was abolished by removal of extracellular Ca^{2+}. The current was markedly reduced in the presence of Ni^{2+} or La^{3+}. The pathway activated by this protocol was permeant to Ba^{2+}, displaying complex permeability characteristics at negative potentials. A small inward Mn^{2+} current consistent with a finite permeability of the pathway to Mn^{2+} was detected. In contrast Ni^{2+} displayed no detectable current carrying ability. Extracellular Na^{+} permeated the pathway in the absence of extracellular Ca^{2+}. Under conditions designed to reduce passive depletion of intracellular Ca^{2+} stores, a Ca^{2+} current indistinguishable from that described above was activated by addition of ionomycin. This observation is consistent with the activation of the Ca^{2+} influx pathway occurring as a result of events associated with depletion of intracellular Ca^{2+} stores. Importantly, application of extracellular Ni^{2+} in the presence of ionomycin irreversibly inhibited the current. The presence of an inwardly rectifying K^{+} current in RBL cells could confound studies of the capacitative Ca^{2+} entry current when recorded using pipette solutions devoid of K^{+} since this current would be inward over the voltage range used to investigate the capacitative Ca^{2+} entry current. This study compares an inward rectifying K^{+} current and the capacitative Ca^{2+} entry current in RBL cells and highlights some similarities and differences between the two currents. The results demonstrate that caution should be exercised in interpreting recordings made using extracellular solutions containing even modest amounts of K^{+} when studying the capacitative Ca^{2+} entry current in RBL cells.

Introduction

An increase in the plasma membrane Ca^{2+} permeability following release of intracellular Ca^{2+}-stores ($Ca^{2+}{}_i$) is a ubiquitous phenomena in nonexcitable cells; a process originally termed ''capacitative'' Ca^{2+} entry; for review *see* [29]. Presently, the mechanism(s) underlying the communication between the intracellular Ca^{2+} store and the plasma membrane is not clearly understood. Numerous mechanisms can been proposed to explain the coupling between the $Ca^{2+}{}_i$-stores and the plasma membrane Ca^{2+} influx pathway including; Ca^{2+} induced Ca^{2+} entry [23, 24, 37], production or release of cytochrome P450 metabolites [1, 2], increases in cyclic GMP [25], physical interactions both directly via inositol receptors [12] and indirectly via cytoskeletal components [29], phosphorylation reactions [13, 14, 32, 33, 35, 36], and the generation of a novel second messenger [29, 30]. Further investigations have implicated cellular high energy phosphate compounds in the activation and/or modulation of this store regulated Ca^{2+} influx pathway [3, 5, 7, 17].

Direct whole-cell patch clamp measurements of a Ca^{2+} current stimulated by release of Ca^{2+} from intracellular stores has been reported in a variety of cell types [8, 10, 15, 27, 34, 37, 43]. Whole-cell patch clamp mea-

Correspondence to: M.J. Mason

surements provide both a direct measure of the net transmembrane current and direct access to the cytosolic environment for investigations of the role of membrane impermeant agents in the activation and/or modulation of the capacitative Ca^{2+} entry current. Such a procedure has been employed to investigate the role of GTP hydrolysis in the activation mechanism in the rat basophilic leukemia cell line RBL-2H3 [5]. Since a full characterization of the current under the ionic conditions employed was not presented and the biophysical properties of Ca^{2+} currents activated by release of intracellular Ca^{2+} stores have been reported to differ according to the cell type and/or recording conditions [10, 15, 36, 41, 43], we have undertaken experiments to isolate and characterize the divalent cation current stimulated by release of Ca^{2+} from intracellular stores in RBL-1 cells.

Under carefully defined ionic conditions designed to optimize detection of the current, a number of interesting findings were noted, including complex permeability characteristics of the pathway to Ba^{2+}, apparent permeability to Mn^{2+}, reversible activation of the current when induced by ionomycin and irreversible inhibition of the ionomycin induced current by Ni^{2+}. Furthermore, we have found that the presence of an inwardly rectifying K^+ current previously reported in rat basophilic leukemia cells [22, 40] makes isolation of the store-regulated Ca^{2+} current difficult when experiments are performed in the presence of extracellular K^+. Moreover, interpretation of results obtained in the presence of extracellular K^+ are further compounded by a dramatic similarity between the inhibitory influence of some divalent cations on the capacitative Ca^{2+} entry current and the inwardly rectifying K^+ current.

Materials and Methods

Reagents

Ionomycin and the cesium salt of 1,2-*bis*-(2-aminophenoxy)ethane-N,N,N′,N′,-tetraacetic acid (BAPTA) were purchased from Calbiochem-Novabiochem (San Diego, CA). (N-2-Hydroxyethylpiperazine-N′-2-ethanesulfonic acid (HEPES) was purchased from Calbiochem-Novachem (San Diego, CA) or Sigma (St. Louis, MO). Potassium methylsulfate was purchased from ICN Biochemicals (Aurora, OH). [Ethyleneglycol-*bis*-(β-aminoethyl)-N,N,N′,N′-tetraacetic acid] (EGTA), Na_2GTP and MgATP were purchased from Sigma (St. Louis, MO), $BaCl_2$, $MnCl_2$, $NiCl_2$, CsOH, gluconic acid, N-methyl-D-glucamine and ethyl alcohol were purchased from Aldrich (Milwaukee, WI). $CaCl_2$, $MgCl_2$, NaCl, KCl, HCl, NaOH, KOH, D-glucose and sucrose were purchased from Fisher (Fairlawn, NJ) or Sigma (St. Louis, MO). Ionomycin was made up as a concentrated stock in ethyl alcohol. All internal and external solutions were stored at −20°C.

Cell Culture

RBL-1 cells were graciously provided by Dr. Stephen Ikeda of the Department of Pharmacology, Medical College of Georgia. Cells were propagated in HEPES-buffered RPMI 1640 (Sigma) containing 25 mM sodium bicarbonate, 100 U/ml penicillin and 100 μg/ml streptomycin (Whitaker, Walkersville, MD) and 10% fetal calf serum (FCS; Whitaker) in an incubator containing a humidified atmosphere of 5%/95% CO_2/air maintained at 37°C. Cells grew as adherent monolayers but continued growth resulted in large numbers of cells detaching and existing in suspension. Cells in suspension were used in all experiments and were used for passaging, thus avoiding potential problems associated with the relatively harsh treatment required to isolate adherent cells.

Solutions

Whole-cell Recordings

Unless indicated, experiments were performed in Na^+-free media. Na^+ was replaced with N-methyl-D-glucamine (NMG). External Ca^{2+}-free solution had the following composition (in mM): 140 NMGGluconate, 16 NMGCl, 1 $MgCl_2$, 10 Glucose, 20 Sucrose, 20 HEPES, pH 7.35 with NMG base. Ca^{2+}-containing solutions were made by omitting NMGCl and adding $CaCl_2$ to maintain a constant extracellular Cl^- concentration. Addition of 8 mM total Ca^{2+} resulted in a free [Ca^{2+}] of 1.5 mM as determined with a Ca^{2+}-selective electrode (Orion 93–20, Boston, MA). $BaCl_2$ and $MnCl_2$ containing solutions were made by equimolar replacement of $CaCl_2$. $LaCl_3$ was added directly to the solution without replacement. For experiments employing Ni^{2+}, the extracellular solution had the following composition (in mM): 128 NMG-Gluconate, 16 NMGCl, 1 $MgCl_2$, 8 $CaGluconate_2$, 10 Glucose, 20 sucrose, 20 HEPES, pH 7.35 with NMG base. Ni^{2+}-containing solution was made by omitting NMGCl and adding 8 mM $NiCl_2$ to maintain a constant extracellular Cl^- concentration. When required, Na^+ was added as the Cl^- salt and replaced $CaCl_2$ to maintain a constant extracellular Cl^- concentration. K^+ was added directly to the external solution as the Cl^- salt with no compensation for added Cl^-.

The standard internal pipette solutions had the following composition (in mM): 85 CsGluconate, 5 NMGCl, 20 Cs_4BAPTA, 2 $MgCl_2$, 30 sucrose, 0.1 Na_2GTP, 10 HEPES, pH 7.4 with CsOH or NMG base.

To inhibit the passive depletion of intracellular Ca^{2+} stores, 5 mM NMGCl was removed and 4 mM $CaCl_2$ and 5 mM MgATP added. This internal was titrated to pH 7.4 with NMG base.

Cell-Attached Recordings

External solution used for cell-attached single K^+ channel recordings had the following composition (in mM): 140 NaCl, 5.4 KCl, 2 $CaCl_2$, 0.8 $MgCl_2$, 15 glucose, 10 HEPES, pH 7.4 with NaOH.

Internal pipette solution used for cell-attached single K^+ channel recordings had the following composition (in mM): 20 KCl, 120 Potassium Methylsulfate, 0.44 EGTA, 3 $MgCl_2$, 30 sucrose, 0.1 Na_2GTP, 4 Na_2ATP, 10 HEPES, pH 7.4 with KOH.

Cell Preparation

Cells were prepared immediately before the experiment by removing 10 ml of culture medium from a flask passaged 24–36 hours prior. The medium containing cells in suspension was centrifuged at 50 × *g* for 3 min and the cells were resuspended in Na^+ medium at 37°C containing (in mM): 140 NaCl, 3 KCl, 1 $CaCl_2$, 1 $MgCl_2$, 10 glucose, 20 HEPES, pH 7.4 with NaOH. Cells were then stored at room temperature (24–26°C). For patch clamp recordings a small aliquot of cells was added directly to a sylgard coated 35 mm plastic culture dish

which formed the foundation of the recording chamber. All experiments were performed at room temperature.

Electrophysiological Recordings

Whole-cell current recordings were made in the tight seal configuration using an Axopatch 200A or 1D patch-clamp amplifier. Amplifier control and data acquisition was controlled by Macintosh based custom software (S3, provided by Dr. Steve Ikeda, Department of Pharmacology, Medical College of Georgia). A holding potential of −40 mV was set following formation of a tight seal and 255 ms ramps from −125 to +60 mV were delivered every 3 sec immediately following break-in. Current records were filtered at 1 kHz and recorded on disk for analysis by commercially available waveform analysis software (Igor, Wavemetrics). Data are presented as ramp *I-V* curves or are plotted as the whole-cell current measured from individual ramps at −120 mV *vs.* time. Current values corresponding to −120 mV are the average of three data points recorded over 2 msec. *I-V* curves are not corrected for a minor junction potential present under the conditions employed (approximately 4 mV). To reduce possible complications caused by changes in ''leak'' current during the course of the experiment, raw whole-cell currents are presented unless otherwise noted.

Single channel currents from cell attached recordings were filtered at 1 kHz, and recorded at 2 kHz in response to voltage ramps of 900 msec duration over the membrane potential range −80 to +80 from resting with a 3-sec stimulus interval.

To minimize K^+ leakage into the chamber, the chamber was connected to ground via an agar bridge made with Hank's balanced salt solution containing 5.4 mM K^+.

Extracellular solution changes were usually made by positioning the cell in close proximity to a gravity fed superfusion device. This device consisted of six individual inflow lines connected to a single common superfusion line which allowed a rapid change from one solution to another without the need to reposition the cell. When the current was activated by ionomycin, solution exchange was achieved by switching between large bore superfusion pipettes placed immediately adjacent to the cell. Although this method prevented any possible activation of the current by trace amounts of ionomycin, it resulted in a slower solution exchange due to reduced solution flow from the pipette tip.

Results

To investigate the characteristics of the Ca^{2+} current activated following release of Ca^{2+} from intracellular stores, we have used RBL-1 cells and experimental solutions designed to facilitate detection of small Ca^{2+} currents and an internal solution designed to passively deplete intracellular Ca^{2+} stores (*see* Materials and Methods). Passive depletion was accomplished by using an internal pipette solution containing in mM; 85 CsGluconate, 5 NMGCl, 20 Cs_4BAPTA, 2 $MgCl_2$, 30 sucrose, 0.1 Na_2GTP, 10 HEPES, pH 7.4 with CsOH or NMG base. Such a solution would be expected to deplete intracellular Ca^{2+} stores in a time dependent fashion due to endogenous release of Ca^{2+} from intracellular stores and the dialysis of the cytosol with an internal solution containing a high concentration of Ca^{2+} chelator.

RBL-1 cells were added to the experimental chamber in an external solution containing in (mM): 140 NMGGluconate, 8 $CaCl_2$, 1 $MgCl_2$, 10 Glucose, 20 Sucrose, 20 HEPES, pH 7.35 with NMG base. Under these conditions free extracellular Ca^{2+} concentration was 1.5 mM as determined with a Ca^{2+}-sensitive electrode. Immediately following break-in, whole-cell currents in response to voltage ramps of 255 msec duration from −125 to +60 mV from a holding potential of −40 mV were recorded every 3 sec. A representative experiment is shown in Fig. 1. Three seconds after initiation of whole-cell recording, little current was detected over the entire voltage range as demonstrated in the inset to Fig. 1 (record 1). This was followed by a marked time-dependent increase of the inward holding current associated with the generation of a curvilinear inward current and a marked shift of the reversal potential to more positive potentials. Trace 2 shows the current recorded 73 seconds after break-in. To demonstrate the kinetics of the generation of the current, the whole-cell current recorded at −120 mV as measured from individual ramps recorded every 3 sec is plotted as a function of time. A steady-state maximum current was recorded after approximately 60 sec. The generation of this inward current and the accompanying marked shift of reversal potential to more positive potentials are consistent with the activation of a Ca^{2+} current.

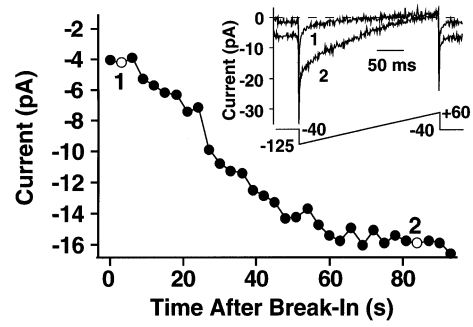

Fig. 1. Time course of the generation of inward whole-cell current following initiation of whole-cell recording in RBL-1 cells with a pipette solution containing a high concentration of BAPTA. Inset. Record 1 shows the whole-cell current recorded 3 sec after initiation of whole-cell recording in the presence of 8 mM total extracellular Ca^{2+} (free $[Ca^{2+}]$ = 1.5 mM) during a 255 msec voltage ramp from −125 to +60 mV from a holding potential of −40 mV. Record 2 shows whole-cell currents recorded in response to the same ramp protocol 84 sec after initiation of whole-cell recording. Records are not leak subtracted. The graph shows the time course of the generation of the whole-cell currents monitored at −120 mV as measured from individual voltage ramps. Open circles labeled 1 and 2 are the current values at −120 mV corresponding to the ramp *I-V* relationships presented in the insert.

To directly test this hypothesis, the sensitivity of this current to changes of extracellular Ca^{2+} concentration was monitored. Rapid changes of external solution were made with a perfusion device capable of perfusing up to six solutions. Following activation of this curvilinear in-

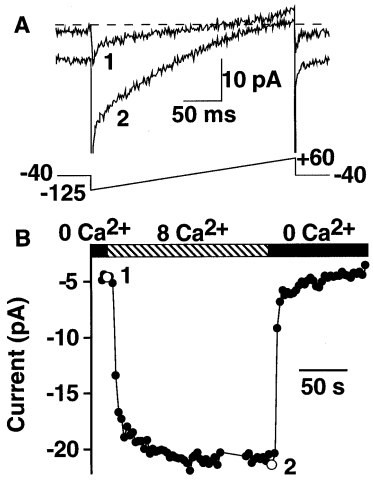

Fig. 2. Ca^{2+} dependence of the whole-cell inward current recorded following dialysis of the cell interior with a high concentration of BAPTA. Panel (*A*) Following generation of the inward current as shown in Fig. 1, changes of extracellular [Ca^{2+}] from 8 mM to 0 were made and whole-cell ramp *I-V* relationships recorded in response to the ramp protocol illustrated. Record 1 and 2 show representative *I-V* relationships in the absence and presence of 8 mM total extracellular Ca^{2+} respectively. Records are not leak subtracted. Panel (*B*) Time course of the changes of whole-cell current recorded at −120 mV as measured from individual voltage ramps applied during rapid changes of total extracellular [Ca^{2+}] as indicated. Concentrations correspond to total Ca^{2+} added (mM) and do not reflect the free concentrations. Open circles labeled 1 and 2 are the current values at −120 mV corresponding to the ramp *I-V* relationships presented in Panel (*A*).

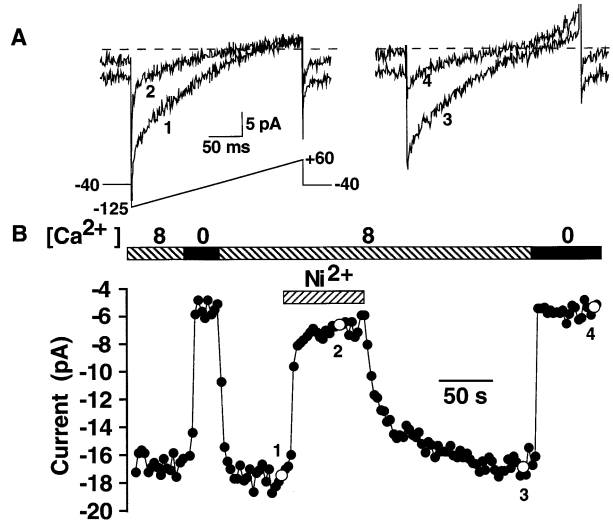

Fig. 3. Block of the inward Ca^{2+} current by extracellular Ni^{2+}. Panel (*A*) Following generation of the inward current by dialysis of the cell interior with a high concentration of BAPTA, changes of extracellular [Ca^{2+}] were made to confirm the Ca^{2+} dependence of the current. Record 1 shows the *I-V* relationship in the presence of 8 mM total Ca^{2+}. Record 2 shows the *I-V* relationship in response to the ramp protocol illustrated in the presence of 8 mM total Ca^{2+} and 8 mM total Ni^{2+}. Record 3 and 4 show representative ramp *I-V* relationships in response to the ramp protocol illustrated in the presence and absence of Ca^{2+} respectively. Records are not leak subtracted. Panel (*B*) Time course of the change of whole-cell current amplitude recorded at −120 mV measured from individual voltage ramps applied during changes of extracellular solution as indicated. Open circles labeled 1–4 are the current values at −120 mV corresponding to the ramp *I-V* relationships presented in Panel (*A*). All concentrations refer to total concentration of divalent ion added (mM) and do not reflect the free concentration.

ward current in the presence of 8 mM total extracellular Ca^{2+} the cell was positioned in the outflow of the perfusion device and solutions of different external Ca^{2+} concentration perfused while recording ramp currents every 3 sec as detailed for Fig. 1. Figure 2*A* shows representative steady state ramp current/voltage (*I-V*) relationships in the presence (record 2) and absence (record 1) of 8 mM total extracellular Ca^{2+} (1.5 mM free [Ca^{2+}] as determined by a Ca^{2+}-sensitive electrode). Addition of extracellular Ca^{2+} was accompanied by a marked increase of the holding current at −40 mV due to the generation of the curvilinear inward current and a marked shift of the reversal potential to more positive values consistent with the presence of a Ca^{2+} conductance. Panel *B* shows the whole-cell current recorded at −120 mV as measured from individual ramps during rapid changes of extracellular [Ca^{2+}]. In the presence of 8 mM Ca^{2+} the steady-state current recorded at −120 mV was −12.9 ± 0.8 pA ($n = 25$). Removal of external Ca^{2+} (nominally Ca^{2+}-free gluconate solution) resulted in a reduction of the current to −4.7 ± 0.4 pA. Thus, the Ca^{2+}-sensitive difference current upon removal of extracellular Ca^{2+} was 8.2 ± 0.7 pA ($n = 25$ cells) at −120 mV. Consistent with the Ca^{2+} dependence of the current, graded changes of extracellular Ca^{2+} concentration were accompanied by graded changes of the magnitude of the inward whole-cell current. A Ca^{2+}-sensitive difference current of 3.3 ± 0.6 pA ($n = 4$ cells) was measured upon removal of 2 mM total extracellular Ca^{2+}. However, the use of gluconate containing solutions with a high Ca^{2+} binding capacity precluded an effective determination of a dose-response relationship for the Ca^{2+} current. The graded increase in inward current was also accompanied by a graded change in the magnitude of the shift of reversal potential to more positive potentials.

The sensitivity of the current to inhibition by extracellular Ni^{2+} was investigated in experiments such as that presented in Fig. 3. Following generation of the inward current, ramp *I-V* relationships were recorded in the absence and presence of 8 mM total extracellular Ca^{2+} to confirm the sensitivity of the current to changes of extracellular Ca^{2+}. The sensitivity of the inward Ca^{2+} current to blockade by Ni^{2+} was investigated by rapidly changing the extracellular solution from one containing 8 mM Ca^{2+} (Panel *A*, record 1) to one containing 8 mM Ca^{2+} and 8 mM Ni^{2+} (Panel *A*, record 2). The inhibitory effect of extracellular Ni^{2+} on the ramp current was evident across all negative voltages and was accompanied

by a marked shift in the reversal potential to more negative potentials. Subsequent removal of extracellular Ni^{2+} resulted in a time-dependent recovery of the inward current (Panel *A*, record 3). Record 4 shows the current in the absence of extracellular Ca^{2+} following recovery from the Ni^{2+} induced block. Fig. 3*B* shows the time course of the changes of whole-cell current recorded at −120 mV, measured from individual ramps, during the solution changes detailed in Panel *A*. In seven cells in this series, removal of 8 mM extracellular Ca^{2+} resulted in a difference current of 7.4 ± 0.8 pA measured at −120 mV. Addition of 8 mM Ni^{2+} in the presence of 8 mM Ca^{2+} resulted in a marked reduction of the inward current recorded at −120 mV. In the seven cells the difference current in the presence of Ni^{2+} was 6.3 ± 0.9 pA. When compared to the difference of current recorded at −120 mV in the presence and absence of extracellular Ca^{2+}, Ni^{2+}, reversibly inhibited the whole-cell current by 85%.

The failure of Ni^{2+} to completely inhibit the inward Ca^{2+}-dependent current measured at −120 mV may arise from incomplete block by Ni^{2+}. Alternatively, the pathway may display some finite degree of permeability to Ni^{2+}. To distinguish between these possibilities we have monitored the effect of extracellular Ni^{2+} on whole-cell ramp currents in the absence of extracellular Ca^{2+}. The sensitivity of the inward current to alterations of extracellular [Ca^{2+}] was first confirmed. Figure 4*A* shows individual ramp *I-V* relationships in the presence (record 1) or absence (record 2) of 8 mM extracellular Ca^{2+}. Removal of extracellular Ca^{2+} resulted in a reduction of the inward current amplitude and a shift of the reversal potential to more negative values consistent with the presence of a Ca^{2+} current. Extracellular solution was then changed to one devoid of added Ca^{2+} and containing 8 mM Ni^{2+} (record 3). No detectable increase of inward current was observed consistent with the inability of Ni^{2+} to permeate the pathway. Superfusion with a solution containing 8 mM Ca^{2+} in the sustained presence of Ni^{2+} resulted in a slow development of a small inward current observable at negative potentials (Panel *A*, record 4) consistent with incomplete block of the Ca^{2+} dependent influx current as reported in Fig. 3. Figure 4*B* shows the time course of the changes of whole-cell current amplitude recorded at −120 mV, measured from individual ramps, during the solution changes detailed in Panel *A*. These data clearly demonstrate that addition of 8 mM Ni^{2+} to the extracellular solution was without a discernable effect on the whole-cell current recorded at −120 mV, consistent with the proposal that the pathway is not permeable to Ni^{2+}. Therefore, the residual current detected in the presence of 8 mM extracellular Ca^{2+} and 8 mM Ni^{2+} is most likely a result of incomplete block by Ni^{2+} of the Ca^{2+}-dependent current rather than a result of a small Ni^{2+} conductance.

Experiments were performed to investigate the inhibitory effect of low concentrations of La^{3+} on the current. La^{3+} induced a dramatic reduction of the amplitude of the inward current across all negative voltages. This reduction of inward current was accompanied by a marked shift of the reversal potential to more negative potentials (*results not shown*). The *I-V* relationship in the presence of La^{3+} was similar to that observed in the absence of extracellular Ca^{2+}. In four experiments in this series, removal of extracellular Ca^{2+} resulted in a difference current of 7.9 ± 0.6 pA at −120 mV, whereas the difference current in the presence and absence of La^{3+} was 7.2 ± 0.8 pA. Thus, when compared to the difference current recorded in the presence and absence of extracellular Ca^{2+} in this cell sample, La^{3+} inhibited by 91.0% the whole-cell current recorded at −120 mV.

The permeability of the pathway to Ba^{2+} was investigated by recording *I-V* ramp relationships in the absence and presence of extracellular Ba^{2+}. Figure 5*A* shows the effect of removal of extracellular Ca^{2+} on the ramp *I-V* relationships (record 1 presence of Ca^{2+}; record 2 absence of Ca^{2+}). After confirming the dependence of the ramp current on extracellular Ca^{2+}, changing from a so-

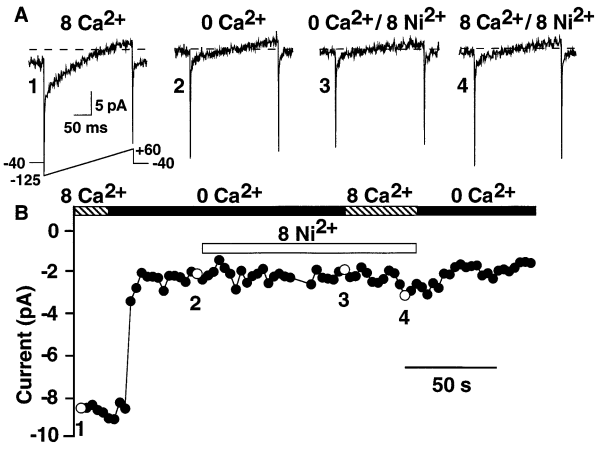

Fig. 4. Effect of extracellular Ni^{2+} on whole-cell current in the absence of extracellular Ca^{2+}. Panel (*A*) Following generation of the inward current, by dialysis of the cell interior with a high concentration of BAPTA, changes of extracellular [Ca^{2+}] were made to confirm the Ca^{2+} dependence of the current. Record 1 and 2 show representative ramp *I-V* relationships in response to the ramp protocol illustrated in the presence and absence of added Ca^{2+} respectively. Record 3 shows a representative *I-V* relationship following the subsequent addition of 8 mM total Ni^{2+} to the extracellular medium. Record 4 shows the *I-V* relationship following the subsequent application of extracellular solution containing 8 mM total Ca^{2+} and 8 mM total Ni^{2+}. Records are not leak subtracted. Panel (*B*) Time course of the change of whole-cell current amplitude recorded at −120 mV measured from individual voltage ramps applied during changes of extracellular solution as indicated. Open circles labeled 1–4 are the current values at −120 mV corresponding to the ramp *I-V* relationships presented in Panel (*A*). All concentrations refer to total concentration of divalent ion added (mM) and do not reflect the free concentration.

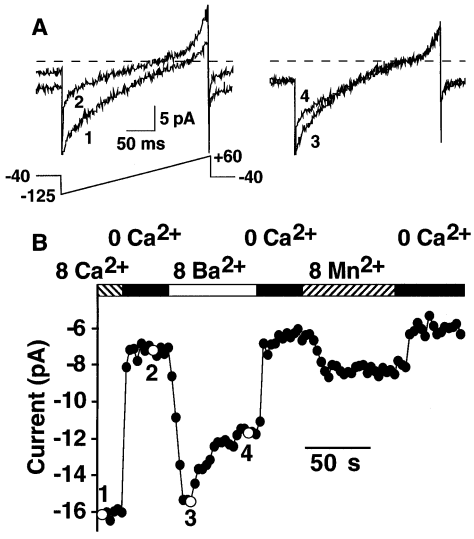

Fig. 5. Permeability of the influx pathway to Ba^{2+} and Mn^{2+}. Following generation of the inward current, by dialysis of the cell interior with a high concentration of BAPTA, changes of extracellular [Ca^{2+}] were made to confirm the Ca^{2+} dependence of the current. Record 1 and 2 show representative ramp *I-V* relationships in response to the ramp protocol illustrated in the presence and absence of Ca^{2+} respectively. Record 3 shows the *I-V* relationship 18 sec after changing from 0 Ca^{2+}-containing solution to one containing 8 mM total Ba^{2+}. Record 4 shows the *I-V* relationship 63 sec after changing to Ba^{2+}-containing solution. Panel (*B*) Time course of the change of whole-cell current amplitude recorded at −120 mV measured from individual ramps during changes of extracellular solution from one devoid of added Ca^{2+} to one containing 8 mM total Ca^{2+}, Ba^{2+} or Mn^{2+} as indicated. Open circles labeled 1–4 are the current values at −120 mV corresponding to the ramp *I-V* relationships presented in Panel (*A*) All concentrations refer to total concentration of divalent ion added (mM) and do not reflect the free concentration.

lution devoid of added Ca^{2+} to one containing 8 mM total Ba^{2+} resulted in a rapid marked increase of the amplitude of the inward current to values approximating that recorded in the presence of 8 mM Ca^{2+}. Record 3 displays the ramp *I-V* relationship recorded 18 sec after addition of Ba^{2+}. Record 4 shows the *I-V* relationship recorded 63 sec after addition of Ba^{2+}. Analysis of the results of seven experiments revealed that the time-dependent reduction of the amplitude of the inward current was confined to potentials more negative than −40 mV. Panel *B* shows the time course of the changes of whole-cell current recorded at −120 mV, measured from individual ramps. It is clear from this experiment that the current recorded at −120 mV during exposure to 8 mM total extracellular Ba^{2+} rapidly declined; reaching a stable plateau value after approximately 1 min. Subsequent removal of Ba^{2+} resulted in a reduction of the inward current recorded at −120 mV of 5.8 ± 1.1 pA ($n = 7$).

In many cells types it has been concluded that the capacitative entry pathway is permeant to Mn^{2+}. Such conclusions are based upon the observation that depletion of intracellular Ca^{2+} stores stimulates Mn^{2+} entry as monitored by the rate of Mn^{2+} quench of intracellularly trapped calcium-sensitive fluorescent indicators. Experiments were undertaken to determine if a Mn^{2+} current was detectable following activation of the Ca^{2+} influx pathway in RBL-1 cells. Whole-cell currents at −120 mV in the presence and absence of 8 mM total extracellular Mn^{2+} were monitored after confirmation of the presence of the Ca^{2+} current. A representative experiment is shown in Fig. 5. Changing from a solution devoid of Ca^{2+} to one containing 8 mM Mn^{2+} resulted in a small but measurable increase of inward current measured at −120 mV. Removal of Mn^{2+} resulted in a reproducible reduction of the inward current recorded at −120 mV of 1.3 ± 0.4 pA ($n = 5$).

It is important to note that the magnitude of the currents measured in the presence of Ba^{2+} and Mn^{2+} in experiments such as those presented in Fig. 5 are not due to run down of the store-regulated conductance as addition of 8 mM Ca^{2+} after Ba^{2+} and Mn^{2+} exposure resulted in a Ca^{2+}-dependent difference current recorded at −120 mV of similar magnitude to that recorded at the beginning of the experiment (*results not shown*).

The selectivity of the pathway for Ca^{2+} over Na^{+} was investigated by comparing the inward current recorded at −120 mV in solutions devoid of added Ca^{2+} containing 16 mM Na^{+} with those recorded in solutions containing 8 mM Ca^{2+} and devoid of Na^{+}. The presence of the rectifying inward current was confirmed by measuring the whole-cell current response to changes in extracellular Ca^{2+} from 8 to 0 mM total Ca^{2+}. Cells were then superfused with solutions devoid of added extracellular Ca^{2+} and ramps from −120 to +60 mV administered while altering the extracellular Na^{+} concentration from 0 to 16 mM. In the absence of added extracellular Ca^{2+}, addition of 16 mM Na^{+} resulted in a small increase of inward current of 0.5 ± 0.2 pA at −120 mV ($n = 5$) (*data not shown*). The difference current in response to changing from 8 mM total Ca^{2+} (1.5 mM free) to 0 added Ca^{2+} was 6.7 ± 0.9 in the same cell population. These data support the hypothesis that the capacitative Ca^{2+} entry pathway in RBL-1 cells is highly selective for Ca^{2+} over Na^{+} in the nominal absence of extracellular Ca^{2+} under the present experimental conditions.

A common characteristic of Ca^{2+}-selective channels is their ability to conduct Na^{+} in the absence of extracellular Ca^{2+}. Experiments were undertaken to investigate the permeability of the pathway to Na^{+} in the absence of extracellular divalents. Extracellular solutions devoid of added Ca^{2+} and Mg^{2+} and supplemented with 1 mM EGTA were used. Under these conditions addition of 16 mM Na^{+} was accompanied by a marked inward current. Figure 6 shows the results of such an experiment. Whole cell ramp currents in the absence of Ca^{2+} and Mg^{2+} and in the absence of extracellular Na^{+} is

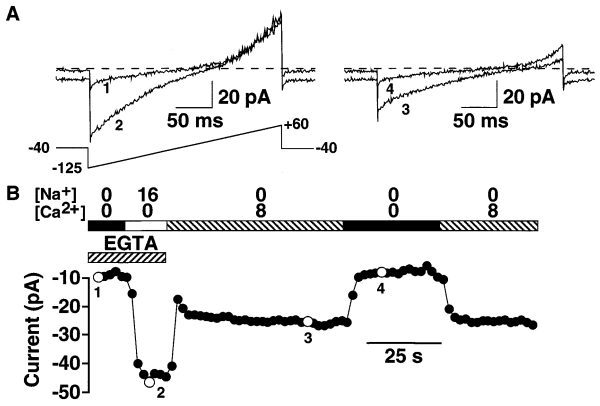

Fig. 6. Na^+ permeability in the absence of extracellular divalents. Following generation of the inward current by dialysis of the cell interior with a high concentration of BAPTA, changes of extracellular $[Ca^{2+}]$ were made to confirm the Ca^{2+} dependence of the current. The cell was then superfused with a solution devoid of added Ca^{2+} and Mg^{2+}, and supplemented with 1 mM EGTA. Record 1 shows a ramp *I-V* relationship under these conditions. Record 2 shows the ramp *I-V* relationship 15 sec following superfusion with a solution containing Na^+. Record 3 shows a representative *I-V* relationship 72 sec after returning to an extracellular solution containing 8 mM total Ca^{2+} and 1 mM total Mg^{2+} in the absence of EGTA. Record 4 shows a typical *I-V* relationship following the subsequent removal of extracellular Ca^{2+} in the sustained presence of Mg^{2+}.

shown in Panel *A* record 1. Substitution of 16 mM NMGCl with NaCl produced a large inward current at negative potentials with no detectable alteration in the outward current component. This increase in inward current was accompanied by a shift in the reversal potential to more positive potentials consistent with an inward Na^+ current. Replacement of extracellular Na with 8 mM total Ca^{2+} in medium containing 1 mM Mg^{2+} resulted in a reduction in both the inward and outward current components of the ramp as evident in record 3. The inward current component was greatly reduced by removal of extracellular Ca^{2+} and was accompanied by a shift in the reversal potential to more positive potentials, consistent with an inward Ca^{2+} current. Our attempts to determine if the outward current was associated with anomalous permeability due to removal of extracellular divalents were thwarted by its lack of stability. In many experiments, the magnitude of the outward current measured in the absence of extracellular Na^+ and extracellular divalents showed rapid and marked fluctuations, making interpretation of alterations in current amplitude induced by changing the extracellular ionic composition difficult. Furthermore, brief exposure to solutions devoid of divalents was often associated with the generation of both large inward and outward currents. While the origin of these currents is unknown, readdition of extracellular Ca^{2+} greatly reduced the currents. Such a finding may be indicative of membrane instability resulting in alterations in leak current or instability of the pipette/membrane seal in the absence of divalents.

Taken in concert, these data support the hypothesis that release of Ca^{2+} from intracellular Ca^{2+} stores activates a highly selective inward divalent cation current. Additionally, in the absence of extracellular Ca^{2+}, the pathway becomes permeant to Na^+. Due to the passive nature of the depletion protocol employed in the patch clamp experiments we cannot unequivocally ascribe the activation of this current to release of Ca^{2+} from intracellular stores. Therefore, to confirm the role of Ca^{2+}-store depletion in activation of this current we have measured whole-cell currents under conditions in which we actively depleted intracellular Ca^{2+} stores. Specifically, we have supplemented the internal solution with 4 mM Ca^{2+} and 5 mM MgATP as described in Materials and Methods. Using this internal solution, whole-cell dialysis did not result in activation of the current for up to 15 min, the longest time interval tested (*results not shown*). Depletion of intracellular Ca^{2+} stores was then induced by application of external solution containing 14 μM ionomycin, applied by lowering a large bore superfusion pipette over the cell. Ionomycin has been previously shown to activate the electrogenic Ca^{2+} influx pathway activated by release of intracellular Ca^{2+} stores in T- and B-lymphocytes, a direct result of the ability of ionomycin to release intracellular stores [16, 20, 40]. A representative experiment utilizing this protocol is shown in Fig. 7. Figure 7*A* shows representative ramp *I-V* relationships before (superfusion with vehicle control solution) and 73 sec after ionomycin addition in the presence of 8 mM total extracellular Ca^{2+}. Addition of vehicle control solution did not significantly influence the basal current. Subsequent application of ionomycin (14 μM) consistently resulted in the rapid generation of an inward current indistinguishable on the basis of its *I-V* relationship from that activated by passive depletion of intracellular stores. The kinetics of the generation of this current measured at −120 mV as taken from the individual voltage ramps is plotted in Fig. 7*B*. In ten experiments ionomycin induced an inward current measured at −120 mV of −10.1 ± 1.2 pA in the presence of 8 mM extracellular Ca^{2+}. Interestingly, removal of the ionomycin pipette resulted in the slow loss of the inward current as shown in Fig. 7*B*. The reversibility of the current appears to be a direct result of removal of the extracellular ionophore and its rapid partitioning out of cellular membranes given that (i) readdition of ionomycin was accompanied by generation of the current (*see* Panel *A* records 3 and 4 for representative *I-V* ramps) and (ii) generation of the current was not observed following exposure to a second superfusion pipette containing control solution. These data are consistent with the requirement for continual application of ionophore for sustained activation of the current under the present conditions. Single cell fluorimetric measurements of $[Ca^{2+}]_i$ have confirmed that ionomycin easily partitions in and out of the membrane

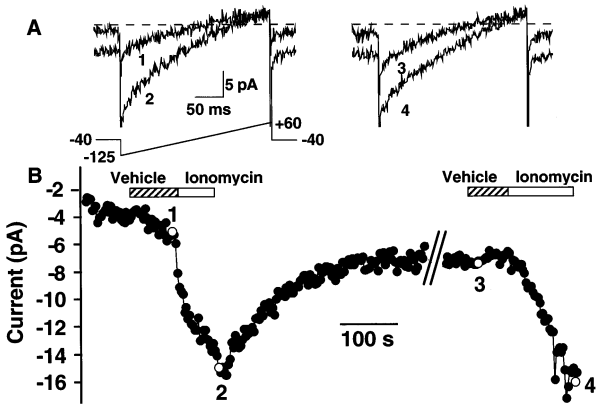

Fig. 7. Ionomycin activation of inward current in the presence of extracellular Ca^{2+}. Panel (*A*) Pipette solutions supplemented with Ca^{2+} and ATP were used to reduce spontaneous activation of the Ca^{2+} current (*see* Materials and Methods). Record 1 shows a representative *I-V* relationship in response to the voltage protocol illustrated, in a cell superfused with solution containing 8 mM total Ca^{2+} and supplemented with ethanol as a vehicle control. Record 2 shows a representative *I-V* relationship approximately 75 sec after application of solution containing 14 μM ionomycin. Record 3 shows a representative *I-V* relationship in control solution approximately 14.5 min after removal or extracellular ionomycin. Record 4 shows a representative *I-V* relationship approximately 2 min after readdition of ionomycin. Panel (*B*) Time course of the change of whole-cell current amplitude recorded at −120 mV measured from individual ramps in response to addition of 14 μM ionomycin as indicated. Break denotes a halt in data collection of approximately 7 min. Open circles labeled 1–4 are the current values at −120 mV corresponding to the ramp *I-V* relationships presented in Panel (*A*) All concentrations refer to total concentration of divalent ion added (mM) and do not reflect the free concentration.

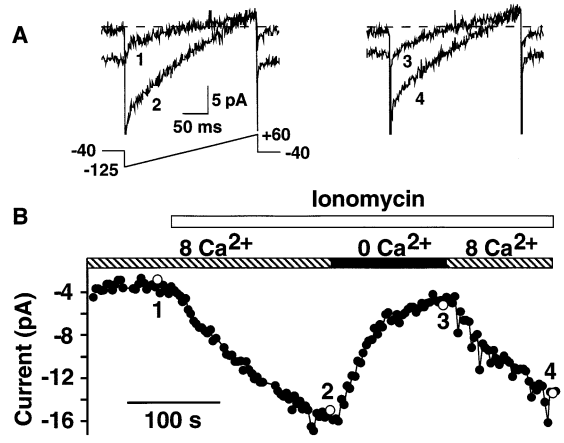

Fig. 8. Ca^{2+} dependence of the ionomycin-induced inward current. Panel (*A*) Pipette solutions supplemented with Ca^{2+} and ATP were used to reduce spontaneous activation of the Ca^{2+} current (*see* Materials and Methods). Record 1 shows a representative *I-V* relationship in response to the voltage protocol illustrated, in a cell superfused with solution containing 8 mM total Ca^{2+} prior to addition of ionomycin. Record 2 shows the *I-V* relationship after the addition of 14 μM ionomycin and maximum generation of the inward current. Records 3 and 4 are *I-V* relationships in the absence and presence of 8 mM total Ca^{2+} respectively. Panel (*B*) Time course of the change of whole-cell current amplitude recorded at −120 mV measured from individual ramps in response to the solutions changes indicated. Open circles labeled 1–4 are the current values at −120 mV corresponding to the ramp *I-V* relationships presented in Panel (*A*). All concentrations refer to total concentration of divalent ion added (mM) and do not reflect the free concentration.

thus requiring sustained application of the ionophore for the maintanence of sustained increases in $[Ca^{2+}]_i$ (*results not shown*).

The Ca^{2+} sensitivity of the ionomycin activated inward current was tested by removing external Ca^{2+} following activation of the current with 14 μM ionomycin. A representative experiment is presented in Fig. 8. Panel *A* shows representative ramp *I-V* relationships before and after ionomycin addition and in the presence and absence of 8 mM extracellular Ca^{2+}. Record 1 shows the whole-cell ramp *I-V* relationship prior to the addition of ionomycin. Record 2 shows the *I-V* relationship after maximal generation of the current in the presence of ionomycin. Removal of Ca^{2+} resulted in a reduction of the amplitude of the current and a shift of the reversal potential to more negative values (record 3). Readdition of Ca^{2+} dramatically increased the magnitude of the inward current (record 4). The mean Ca^{2+}-sensitive difference current in 5 cells was −10.0 ± 1.1 pA. The time course of the changes of whole-cell current recorded at −120 mV is shown in Panel *B.*

We have investigated the effect of extracellular Ni^{2+} addition on the current activated by ionomycin. The results of a representative experiment are presented in Fig. 9. Panel A shows the whole cell ramp current immediately prior to application of 14 μM ionomycin (record 1) and after maximal activation of the current (record 4). Consistent with the effect of Ni^{2+} on the Ca^{2+} current activated by passive depletion, application of extracellular Ni^{2+} in the sustained presence of Ca^{2+} and ionomycin dramatically inhibited the inward current (record 3). This inhibition was accompanied by a shift in the reversal potential to more negative potentials. In marked contrast to the effects of Ni^{2+} on the current activated by passive depletion, inhibition of the ionomycin-induced current was irreversible (record 4). The kinetics of the generation of the current measured at −120 mV following application of ionomycin and the irreversible inhibition of the current by Ni^{2+} application are shown in Panel *B.* The difference current measured at −120 mV in the presence and absence of Ni^{2+} was 7.1 ± 2.8 pA ($n = 4$ cells).

Taken in concert, active depletion of intracellular Ca^{2+} stores by application of ionomycin results in the activation of a rectifying Ca^{2+} sensitive inward current dramatically inhibited by 8 mM extracellular Ni^{2+}. These characteristics are indistinguishable from the current generated following whole-cell dialysis with high con-

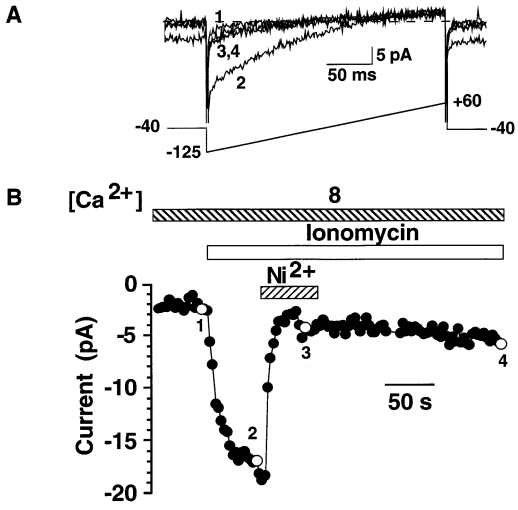

Fig. 9. Irreversible block by Ni^{2+} of the inward Ca^{2+} current activated by ionomycin. Panel (*A*) Pipette solutions supplemented with Ca^{2+} and ATP were used to reduce spontaneous activation of the Ca^{2+} current (*see* Materials and Methods). Record 1 shows a representative *I-V* relationship in response to the voltage protocol illustrated, in a cell superfused with solution containing 8 mM total Ca^{2+}, prior to addition of ionomycin. Record 2 shows the *I-V* relationship after the addition of 14 μM ionomycin and generation of the inward current. Record 3 is a representative ramp *I-V* relationship following superfusion with solution containing 8 mM total Ni^{2+} in the presence of 8 mM total Ca^{2+} and 14 μM ionomycin. Record 4 is a representative *I-V* relationship 190 sec after superfusion with Ni^{2+}-free solution. Panel (*B*) Time course of the change of whole-cell current amplitude recorded at −120 mV measured from individual ramps in response to the solution changes indicated. Open circles labeled 1–4 are the current values at −120 mV corresponding to the ramp *I-V* relationships presented in Panel *A*. All concentrations refer to total concentration of divalent ion added (mM and do not reflect the free concentration.

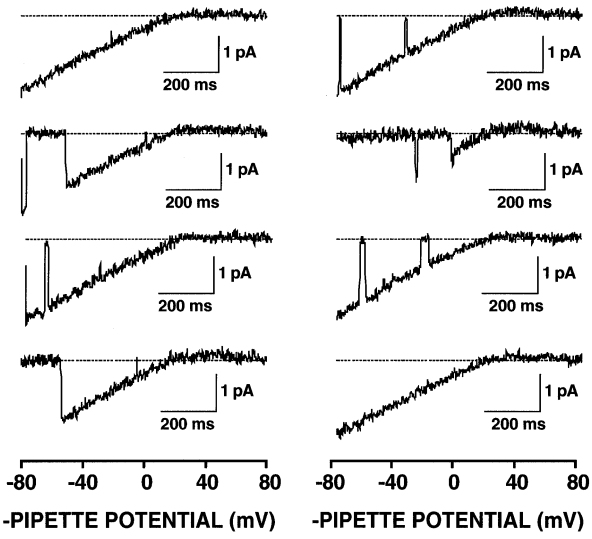

Fig. 10. Cell-attached patch recordings of single channel currents of the inwardly rectifying K^+ current in response to 900 msec voltage ramp from −80 to +80 mV. Records have been corrected for linear leakage estimated from a fit of the current during closed intervals. The cell was bathed in normal extracellular solution containing 5.4 mM K^+. The pipette solution contained 140 mM K^+. Records were recorded at 1 KHz. Inward currents are negative and the dotted line shows the zero current level. The potentials are shown as applied membrane potentials, i.e., negative pipette potential.

centrations of the Ca^{2+} chelator BAPTA and are consistent with the hypotheses that activation of the current is a direct result of passive depletion of Ca^{2+}_i stores.

The existence of an inwardly rectifying K^+ current has previously been reported in cultured RBL cells [22, 40]. It is unlikely that the existence of such a current could influence or contaminate the present results, given that these experiments were performed in the absence of extracellular K^+. However, experiments were undertaken to investigate the possibility that the inward Ca^{2+} current arises as a result of a small permeability of the inward rectifier to Ca^{2+} in the absence of extracellular K^+.

The presence of an inwardly rectifying K^+ current was confirmed in cell attached patch experiments. Cells were bathed in normal Na^+ solution containing 5.4 mM K^+ and 2 mM Ca^{2+} to maintain a normal transmembrane potential. A high K^+ containing pipette solution was used (*see* Materials and Methods) and 900 msec ramps delivered from −80 to +80 mV from a holding potential of 0 mV were initiated after formation of a high resistance seal. Figure 10 shows representative ramp current traces recorded under these conditions. Record 1 reveals an inwardly rectifying current displaying little outward current component. Single-channel closing events are evident in subsequent records. All records were leak subtracted by estimating the leakage current by linear regression from the closing events. The estimated single channel conductance measured from steady-state single channel *I-V* curves or single openings from a ramp protocol in a single experiment was 33 ± 1.6 pS, a value not that different from previously reported values in RBL-2H3 cells [22, 40].

Experiments were undertaken to confirm the K^+ sensitivity of this current and to define the current/voltage characteristics under the experimental conditions employed for the detection of the Ca^{2+} current activated by release of intracellular Ca^{2+} stores. Figure 11 shows the results of a representative experiment. A K^+-free pipette solution identical to that employed for the detection of the Ca^{2+} current was used. Where indicated, the external solution, which was identical to that employed for detection of the Ca^{2+} current, was supplemented with 5 mM K^+ (*see* Materials and Methods). Representative whole-cell current records in response to 255 msec ramps from the indicated potentials are shown in the presence or absence of 5 mM extracellular K^+. Panel *B* shows the whole-cell current recorded at −120 mV during changes in extracellular K^+ concentration. It is clear from these

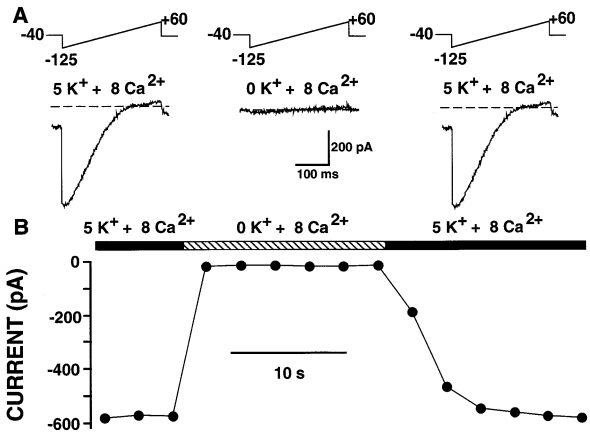

Fig. 11. K^+ sensitivity of the inwardly rectifying K^+ current. Panel (*A*) Representative *I-V* relationship in response to the voltage protocol illustrated in the presence and absence of 5 mM external K^+ as indicated. External solution was that used to record the inward Ca^{2+} current supplemented with 5 mM K^+. Panel (*B*) Time course of the change of whole cell current amplitude recorded at −120 mV measured from individual voltage ramps applied during changes of extracellular solution as indicated. Divalent ion concentrations refer to total concentration (mM) and do not reflect the free concentration.

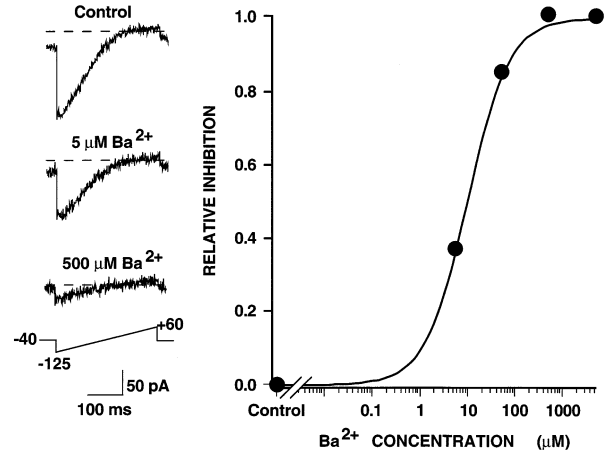

Fig. 12. Ba^{2+} sensitivity of the inwardly rectifying K^+ current. Panel (*A*) Representative *I-V* relationships in response to the voltage protocol illustrated in the absence of added Ba^{2+} and in the presence of 5 μM and 500 μM external Ba^{2+}. External solution was that used to record the inward Ca^{2+} current supplemented with 5 mM K^+ and Ba^{2+} as indicated. Panel (*B*) Concentration response relationship of the whole cell current recorded at −120 mV measured from steady-state *I-V* relationships following changes of extracellular Ba^{2+} concentration as indicated. Divalent ion concentrations refer to total concentration added (mM) and do not reflect the free concentration. The solid line is a least squares fit of the data to a single site binding isotherm.

experiments that a K^+ dependent inwardly rectifying current measuring approximately 600 pA at −120 mV dominates the current record under these conditions.

Experiments were undertaken to investigate the sensitivity of this K^+ current to Ba^{2+} and Ni^{2+}. Figure 12 shows the results of a representative experiment. A K^+-free pipette solution identical to that employed for the detection of the Ca^{2+} current was used. Normal external solution used for measurements of the Ca^{2+} current were supplemented with 5 mM K^+. Representative whole-cell current records in response to 255 msec ramps from the indicated potentials are shown in the absence or presence of increasing concentrations of extracellular Ba^{2+}. The graph shows a typical concentration response curve for Ba^{2+} induced inhibition of the inwardly rectifying K^+ current measured at −120 mV. The half maximal inhibition induced by Ba^{2+} was 6.9 ± 1.7 μM ($n = 3$). The inwardly rectifying K^+ current was also inhibited by extracellular Ni^{2+} and Mn^{2+} (*results not shown*).

Discussion

Modulation of the Ca^{2+} permeability of the plasma membrane by the Ca^{2+} level in intracellular compartments is virtually a universal phenomena in nonexcitable cells. The characteristics of this electrogenic pathway, on the other hand, are far less universal with marked differences reported in permeability to divalent ions and monovalent cations, and the ability to resolve single-channel events. With these differences in mind and the knowledge that an extensive characterization of the current activated by release of intracellular Ca^{2+} stores in RBL-1 cells has yet to be presented we undertook experiments to define the biophysical characteristics of this current under carefully defined ionic conditions.

Consistent with the modulation of the plasma membrane Ca^{2+} permeability by the Ca^{2+} content of intracellular stores we have found that an inwardly rectifying current spontaneously activates in a time dependent manner following initiation of whole-cell current recordings when the pipette solution contains high concentrations of the Ca^{2+} chelator BAPTA. Such conditions are expected to scavenge cytosolic Ca^{2+} and induce depletion of intracellular Ca^{2+} stores.

The Ca^{2+} dependence of the current was confirmed by manipulating the extracellular Ca^{2+} concentration. The magnitude of the current increased in a dose-dependent fashion with increases of extracellular Ca^{2+}. The use of external solutions containing 140 mM gluconate, an anion substitute with a marked affinity for divalent cations, precluded a comprehensive investigation of the quantitative dependence of the inward current upon external Ca^{2+} concentrations. However, the present data shows a clear graded increase in current when external Ca^{2+} is raised from 0 to 2 or 8 mM total concentration. The increase of current was accompanied by a Ca^{2+} concentration dependent shift of the reversal potential of the raw whole-cell current recordings towards more positive values, consistent with increased Ca^{2+}

conductance. Alterations of extracellular Cl^- concentrations had no effect on the magnitude or reversal potential, precluding the possibility that the inward current induced by depleting intracellular stores is carried by Cl^- (*results not shown*).

The current activated in the present experiments displays a high degree of selectivity for Ca^{2+} over Na^+, with no measurable increase of inward current when 12 mM Na^+ was added to an extracellular solution containing 2 mM total extracellular Ca^{2+}. Interestingly, a small increase of inward current was recorded in the absence of added extracellular Ca^{2+}. Removal of extracellular divalents frequently induced large inward and outward currents. The magnitude and reversal potential of these currents was unresponsive to extracellular ionic substitution consistent more with an instability of the membrane or the pipette/membrane seal rather than the activation of a physiologically relevant conductive pathway. However, in a number of experiments removal of extracellular divalents and addition of EGTA was not immediately accompanied by these currents. Under these conditions a Na^+ dependent inward current such as that presented in Fig. 6 was detected. These data are consistent with the capacitative Ca^{2+} entry current in the cultured T-lymphocyte cell line Jurkat and mast cells which have been reported to display marked Na^+ permeability when Ca^{2+} was buffered to low levels [11, 27], a phenomena most likely reflecting anomalous permeability.

Spontaneous activation of the inwardly rectifying Ca^{2+} current following initiation of whole-cell conditions could be inhibited by addition of Ca^{2+} and ATP to the pipette solution; preventing spontaneous depletion of intracellular Ca^{2+} stores. Under these conditions a brief application of a high concentration of ionomycin induced an inward current indistinguishable from the inward current activated by passive depletion with regards to its *I-V* relationship, sensitivity to alterations of extracellular Ca^{2+} concentration and inhibitory sensitivity to extracellular Ni^{2+}. Ionomycin has been shown previously to activate the capacitative Ca^{2+} influx pathway in T- and B-lymphocytes, a direct result of release of intracellular Ca^{2+} stores [1, 16, 18, 39]. Taken in concert, these data support the conclusion that release of intracellular Ca^{2+} stores either passively by scavenging intracellular Ca^{2+} or actively by ionophoretic transport of Ca^{2+} across the endosomal membrane induces the activation of a Ca^{2+}-selective inward current.

Ionomycin has previously been used to activate the capacitative Ca^{2+} entry current in mast cells [10], Jurkat cells [27] and an inward current reported to be the capacitative Ca^{2+} entry current in RBL-2H3 cells [5]. Activation of the current by ionomycin application in the present experiments reversed upon removal of ionophore (*see* Fig. 8). Although not previously reported, such an effect is not surprising if it is assumed that ionomycin can readily partition in or out of cellular membranes, an assumption confirmed in single cell fluorimetric measurements of $[Ca^{2+}]_i$ [21]. With this finding in mind, the presence of ATP in the pipette solution provides the necessary energy source for endosomal Ca^{2+}-ATPase activity. As a direct result, removal of extracellular ionomycin and subsequent wash out of ionomycin from the endosomal membranes would allow for the refilling of the intracellular Ca^{2+} stores. If Ca^{2+} loss from the endosomal stores is the trigger to activation of the inward current then repleting the stores should induce deactivation consistent with our findings. Reapplication of ionomycin in the present experiments was followed by the re-activation of the current, thus (i) ruling out events associated with inactivation of the current while (ii) providing further support for the modulation of the plasma membrane Ca^{2+} permeability by the Ca^{2+} content of endosomal Ca^{2+} stores. These experiments warrant exercising caution when activating this current by brief application of ionophore, particularly when utilizing ionomycin in investigations of the inactivation characteristics of the current.

When used at high concentrations, extracellular Ni^{2+} is known to be an effective, reversible blocker of the Ca^{2+} influx pathway activated by depletion of intracellular Ca^{2+} stores [16, 39, 43]. In contrast, when applied in the presence of ionomycin, the block induced by extracellularly applied Ni^{2+} was found to be irreversible within the time frame of these experiments. Under normal conditions, plasma membranes are relatively impermeant to Ni^{2+}. However, in the presence of ionomycin, Ni^{2+} is transported across the plasma membrane as evidenced by the ability of ionomycin application in the presence of Ni^{2+} to dramatically increase the rate of quench of intracellularly trapped fura2 (*data not shown*). It is unlikely that the reduction of the current in the presence of Ni^{2+} is due to impairment of the ability of ionomycin to deplete the Ca^{2+} stores since the lack of reversibility of the inhibition induced by Ni^{2+} in the presence of ionmycin was also detected in experiments using pipette solution devoid of Ca^{2+} and ATP; an internal solution which by itself, passively depletes the Ca^{2+} stores and activates the current (*results not shown*). Recent work from our laboratory has demonstrated that BAPTA can effectively scavenge Ni^{2+} [21]. Therefore, given that the whole cell configuration provides an effectively infinite BAPTA reservoir, the data is consistent with binding of Ni^{2+} to a high affinity intracellular site.

The present experiments have confirmed complex Ba^{2+} permeability characteristics previously reported in RBL-2H3 cells [9]. Specifically, we have found that the current carried by Ba^{2+} inactivates in a time-dependent fashion. Interestingly, this inactivation occurs only at potentials more negative than −60 mV. It is important to note that changing solutions from 0 Ca^{2+} to 8 mM Ca^{2+}

revealed no inactivation characteristics when monitored at −120 mV. Furthermore, changing the extracellular solution from one containing 8 mM Ca^{2+} to 8 mM Ba^{2+} showed no evidence of a transient increase of current but rather showed a rapid reduction of current to a plateau value similar to that shown in Fig. 5 (*results not shown*). As noted above, a manuscript detailing a similar complex Ba^{2+} conductance pattern in RBL-2H3, mast and Jurkat cells has been published since the completion of the present work [9]. The author details complex multiphasic changes of whole-cell current following exchange of extracellular Ca^{2+} for Ba^{2+}. A model was proposed whereby Ca^{2+} influences the conductance of the pathway by three distinct mechanisms including (i) an effect similar to the one-site Ca^{2+} binding model proposed for voltage-operated Ca^{2+} channels (ii) an action responsible for Ca^{2+} dependent inactivation and (iii) a Ca^{2+} requirement for the functional expression of a permeant pathway [9]. A Ca^{2+} requirement for the functional expression of a permeant pathway has been used to explain the inactivation effect observed in the presence of Ba^{2+}, inasmuch as the washout of extracellular Ca^{2+} following Ba^{2+} addition results in the accompanying loss of a functional pathway and a detectable decline of the Ba^{2+} current recorded at negative potentials. In contrast, the inactivation of the Ba^{2+} current recorded in the present experiments is observed after exposure to Ca^{2+} free gluconate solutions (Fig. 5). Thus, to explain the present results by a similar mechanism, it must be assumed that Ca^{2+} is tightly bound and requires extended time intervals for displacement from binding sites or that Ba^{2+} displaces residual bound Ca^{2+}. Alternatively it can be proposed that Ba^{2+} binding directly modulates the conductance of the pathway via negative feedback. Further experiments are required to distinguish between these two mechanisms.

Rapid Ca^{2+}-dependent inactivation of the current occurring over the millisecond time scale has been reported in Jurkat and mast cells in response to hyperpolarizing pulses [10, 11, 44]. Inactivation in Ba^{2+}-containing solutions is distinguished from Ca^{2+} dependent inactivation by its kinetics, with inactivation in Ba^{2+}-containing solutions occurring over tens of seconds.

Mn^{2+} permeability through the capacitative Ca^{2+} influx pathway has been proposed on the basis of the quench of intracellular fluorescent Ca^{2+} indicators and has been used extensively by our laboratory during investigations of the capacitative entry pathway in rat thymic lymphocytes [18, 19, 20]. Using these techniques and in agreement with a recent report in RBL-2H3 cells [4], we have confirmed that depletion of intracellular Ca^{2+} stores by addition of the endosomal Ca^{2+} ATPase inhibitor thapsigargin stimulates Mn^{2+} influx in RBL-1 cells (*data not shown;* Mason & Mahaut-Smith [19]). Electrophysiological experiments were undertaken in an attempt to further investigate the permeability of this pathway to Mn^{2+} in RBL-1 cells following depletion of intracellular Ca^{2+} stores by passive depletion. A small but reproducible inward current was measured at −120 mV in solution containing 8 mM Mn^{2+} and devoid of Ca^{2+} following depletion of intracellular Ca^{2+} stores. This increase of inward current at −120 mV was accompanied by a small shift of the reversal potential towards more positive potentials consistent with the pathway displaying a measurable permeability to Mn^{2+} (*data not shown*). This increase of current was reversible, displaying a difference current upon removal of extracellular Mn^{2+} of 1.3 ± 0.4 pA at −120 mV ($n = 5$). While these results are consistent with the capacitative entry pathway displaying a small permeability to Mn^{2+}, alternative explanations must be entertained. It can be proposed that the apparent inward Mn^{2+} current arises from the modulation of the leak current by the addition of extracellular Mn^{2+}. This is an important point in the light of the observation that in the absence of divalent ions (Mg^{2+} excluded from this discussion), an outward current at positive potentials is frequently observed in ramp records. While the origin of this current is presently unclear, we have found that extracellular addition of Ni^{2+}, Mn^{2+}, Ba^{2+} or Ca^{2+} effectively reduces this outward current component of the ramp. If this is indicative of an outward current contribution to the whole-cell leak current across all ramp voltages (Cs^{+} for example) then inhibition of this outward current component would appear as an apparent inward current. As a result of this discussion it could be proposed that the effect of Mn^{2+} addition is not a direct result of an inward Mn^{2+} current but rather of inhibition of an outward component of the leak current. To address this hypothesis we have contrasted the effects of Mn^{2+} and Ni^{2+} addition upon the whole-cell ramp current monitored in the absence of extracellular Ca^{2+}. As evident from Fig. 4 (records 2 *vs.* 3), addition of 8 mM Ni^{2+} results in a small inhibition of the outward current component of the ramp with no detectable increase of inward current measured at −120 mV (Panel *B*). This is in marked contrast to the effect of Mn^{2+} addition discussed above and supports the conclusion that the inward current detected is a result of inward Mn^{2+} permeation. It is also conceivable that Mn^{2+} is permeating a pathway distinct from the capacitative Ca^{2+} entry pathway; for example a pathway contributing to the leak current. Since the leak current that generates during dialysis of the cell interior is larger than the Mn^{2+} current under investigation it is difficult to unequivocally ascribe the presence of the Mn^{2+} current to depletion of intracellular Ca^{2+} stores rather than to a component of the leak current that generates in parallel with store depletion. However, given that depletion of intracellular Ca^{2+} stores by addition of endosomal Ca^{2+} ATPase inhibitors stimulates Mn^{2+} entry [4, Mason & Mahaut-Smith; *data not shown*]

it is reasonable to propose that the Mn^{2+} current observed after passive depletion of the Ca^{2+} stores in the present experiments underlies this observation.

It has been shown that store regulated calcium channels display a finite permeability to Mn^{2+} [5]. These authors showed that Mn^{2+} carried only 10% of the current carried by Ca^{2+} even at a 10-fold higher concentration, suggesting a considerably lower permeability of these channels to Mn^{2+} compared to Ca^{2+}. Applying a similar treatment to our data, and using a free Ca^{2+} concentration of 1.5 mM as determined with a Ca^{2+}-sensitive electrode and a free Mn^{2+} concentration of 8 mM, assuming negligible Mn^{2+} binding to gluconate, we determined that Mn^{2+} carried approximately 16% of the current (measured at −120 mV) carried by Ca^{2+} at a 5-fold higher concentration. Thus, the Mn^{2+} permeability demonstrated in this report appears to be at least three times greater than that reported in rat peritoneal mast cells [5]. While it is clear that the permeability of the pathway to Mn^{2+} is low, this detectable permeability would be expected to be adequate to account for the observations of Mn^{2+} stimulated uptake following depletion of Ca^{2+} stores in experiments utilizing Ca^{2+}-sensitive fluorescence indicators.

Due to the presence of an inwardly rectifying K^+ current in RBL cells [22, 40] isolation and characterization of the capacitative Ca^{2+} entry current was performed in the absence of intracellular and extracellular K^+. The possibility that the rectifying inward Ca^{2+} current investigated in the present experiments was a result of a small Ca^{2+} permeability through the inward rectifying K^+ channel in the absence of K^+ is highly unlikely given that Ba^{2+} is a potent blocker of the K^+ current yet is a charge carrier through the pathway activated by release of Ca^{2+} from intracellular stores (Fig. 5). However, the significance of investigating the capacitative entry currents under the absence of K^+ is borne out by the similarity of the *I-V* relationship of these distinct currents under the whole-cell conditions employed in the present investigations. While the magnitude of the current in the presence of 5 mM extracellular K^+ and no K^+ in the pipette solution distinguishes it from the capacitative entry current, care should be exercised to ensure that extracellular solutions are not contaminated by modest levels of K^+ where the magnitude of the current cannot be used to distinguish these currents. Difficulty distinguishing between these currents is further exacerbated by the similarity between the blocking effect of extracellular Ni^{2+} on both currents (*data not shown*).

Activation of the capacitative Ca^{2+} current in RBL-2H3 cells has been reported to require a diffusible cytosolic factor, possibly a small GTP-binding protein, that washes out in a time dependent manner when dialyzing cells in the whole-cell configuration [5]. This conclusion is based upon the observation that the magnitude of the capacitative Ca^{2+} entry current is reduced in proportion to the time of whole-cell dialysis prior to activation of the current with ionomycin. However, these experiments were performed in the presence of 2.8 mM extracellular K^+ and with pipette solutions devoid of K^+. These conditions are similar to those employed in the experiments depicted in Figs. 11 and 12 where the majority of the inward current recorded during ramps from −100 to +100 mV is carried by the inwardly rectifying K^+ current. This is important in the light of the fact that analysis of the activation kinetics undertaken by the authors was based upon the magnitude of the ramp currents recorded at −40 mV, a potential that would most certainly be contaminated by a contribution from the inwardly rectifying K^+ current. Furthermore, the run-down phenomena attributed to washout of a small GTP-binding protein required for the activation of the capacitative entry current is reminiscent of that previously reported for the inwardly rectifying K^+ current in RBL-2H3 cells [22, 40]. Therefore, given the presence of the inwardly rectifying K^+ current in RBL cells and the similarity of the voltage dependence of the current, it is not prudent to ascribe the inactivation phenomena reported by Fasolato and coworkers [5] to the washout of a diffusible cytosolic factor required for the activation of the capacitative Ca^{2+} entry current. A clear demonstration of the Ca^{2+} dependence of the current recorded in their experiments would have obviated the concerns arising from the present discussion.

This concern is further augmented by recently published work from the same laboratory [26]. In these experiments the authors have been unable to demonstrate the time-dependent washout of the Ca^{2+} current previously published by their laboratory [5]. The authors have brought to light two differences in an effort to reconcile these diametrically opposed results. First, EGTA was used to buffer $Ca^{2+}{}_i$ while BAPTA was used in the original report demonstrating a time dependent washout of a signaling molecule required for the activation of the Ca^{2+} current. Second, the use of higher ATP concentrations was postulated as another source of the discrepancy. While these differences may underly this discrepancy, in this most recent report, precautions were also taken to minimize the contribution of the inwardly rectifying K^+ channel to the measured current. This was accomplished by both including high K^+ concentrations in the pipette solution and supplementing the extracellular solution with 10 mM CsCl, a potent inhibitor of the inwardly rectifying K^+ channel at this concentration. As a result of these manipulations, little inward K^+ current would be detected over the voltage range investigated. While it is not possible to unequivocally ascribe the lack of a time-dependent washout to experimental conditions that minimize the inwardly rectifying K^+ current, such a proposal should be seriously considered.

The characteristics of the current isolated in the present experiments are dramatically distinct from membrane currents activated by release of intracellular Ca^{2+} stores in other tissues [8, 15, 36, 41]. In cultured human endothelial cells and mouse pancreatic β cells release of intracellular Ca^{2+} stores by addition of the endosomal Ca^{2+}-ATPase inhibitor thapsigargin induced the activation of a nonselective cation current [8, 41]. In contrast, single-channel events associated with activation of a highly selective Ca^{2+} channel have been reported following release of intracellular Ca^{2+} stores in cultured epidermal cells and bovine aortic endothelial cells [15, 36]. Interestingly, the channel in cultured epidermal cells was far more permeant to Ba^{2+} than Ca^{2+}, a characteristic shared with many types of voltage-activated Ca^{2+} channels. In contrast, the Ca^{2+} current isolated in RBL-1 cells bears a strong similarity to Ca^{2+} currents previously reported in mast cells, Jurkat cells and megakaryocytes [10, 11, 27, 34, 43, 44]. The Ca^{2+} current activated by release of intracellular Ca^{2+} stores in these cells displays an apparently higher selectivity for Ca^{2+} over Ba^{2+} and a low single-channel conductance evident by the lack of detectable single-channel events (*unpublished observations*). Furthermore, the pathway displays no significant permeability to Na^+ in the presence of extracellular Ca^{2+}, a result consistent with the findings reported for mast cells, Jurkat cells and megakaryocytes [10, 11, 27, 34, 43, 44].

The current activated in the present experiments bears similarity to the current activated by antigenic stimulation of RBL-2H3 cells [42]. Both conductances display inward rectification, are inhibited by extracellular La^{3+}, are only marginally permeant to Na^+ in the nominal absence of Ca^{2+} and appear to be activated by depletion of intracellular stores. In contrast to the present results, the current activated by antigen was more permeant to Ba^{2+} at negative potentials, a result of a marked rectification of the current at negative potentials. Interestingly, BAPTA loading reversed the permeability sequence of the current activated by antigen, resulting in Ca^{2+} being more permeant than Ba^{2+}. Without *I-V* relationships for the current in the presence of cytosolic BAPTA further detailed comparisons of the currents are not possible.

It is clear from this discussion that release of intracellular Ca^{2+} stores can induce dramatic alterations in the permeability characteristics of the plasma membrane. Whether the differences between biophysical characteristics arise from distinct families of membrane-spanning proteins or as a result of tissue specific modulation of a single family of proteins is presently unclear.

This work was supported by grants to M.J.M. from the Louisiana Education Quality Support Funds (LEQSF (1993-96)-RD-A31) and from the American Heart Association, Louisiana Affiliate (LA-93-GB-16).

References

1. Alvarez, J., Montero, M., García-Sancho, J. 1991. Cytochrome P-450 may link intracellular Ca^{2+} stores with plasma membrane Ca^{2+} influx. *Biochem. J.* **274:**193–197
2. Alvarez, J., Montero, M., García-Sancho, J. 1992. Cytochrome P-450 may regulate plasma membrane Ca^{2+} permeability according to the filling state of the intracellular Ca^{2+} stores. *FASEB J.* **6:**786–792
3. Bird, G. St. J., Putney, J.W. Jr. 1993. Inhibition of thapsigargin-induced calcium entry by microinjected guanine nucleotide analogues. *J. Biol. Chem.* **268:**21486–21488
4. Falcone, D., Fewtrell, C. 1995. Ca^{2+}-ATPase inhibitor, cyclopiazonic acid releases Ca^{2+} from intracellular stores in RBL-2H3 mast cells and activates a Ca^{2+} influx pathway that is permeable to sodium and manganese. *J. Cell. Physiol.* **164:**205–213
5. Fasolato, C., Hoth, M., Penner, R. 1993. A GTP-dependent step in the activation mechanism of capacitative calcium influx. *J. Biol. Chem.* **268:**20737–20740
6. Fasolato, C., Hoth, M., Penner, R. 1993. Multiple mechanisms of magnanese-induced quenching of fura-2 fluorescence in rat mast cells. *Pfluegers Arch.* **423:**225–231
7. Gamberucci, A., Innocenti, B., Fulceri, R., Bànhegyi, G., Giunti, R., Pozzan, T., Benedetti, A. 1994. Modulation of Ca^{2+} influx dependent on store depletion by intracellular Adenine-Guanine nucleotide levels. *J. Biol. Chem.* **269:**23597–23602
8. Gericke, M., Droogmans, G., Nilius, B. 1993. Thapsigargin discharges intracellular calcium stores and induces transmembrane currents in human endothelial cells. *Pfluegers Arch.* **422:**522–527
9. Hoth, M. 1995. Calcium and barium permeation through calcium release-actived calcium (CRAC) channels. *Pfluegers Arch.* **430:**315–322
10. Hoth, M., Penner, R. 1992. Depletion of intracellular calcium stores activates a calcium current in mast cells. *Nature* **355:**353–356
11. Hoth, M., Penner, R. 1993. Calcium release-activated calcium current in rat mast cells. *J. Physiol.* **465:**359–386
12. Irvine, R.F. 1990. ''Quantal'' Ca^{2+} release and the control of Ca^{2+} entry by inositol phosphates-a possible mechanism. *FEBS Lett.* **263:**5–9
13. Jenner, S., Farndale, R.W., Sage, S.O. 1994. The effect of calcium-store depletion and refilling with various bivalent cations on tyrosine phosphorylation and Mn^{2+} entry in fura-2 loaded human platelets. *Biochem. J.* **303:**337–339
14. Lee, K-M., Toscas, K., Villereal, M.L. 1993. Inhibition of bradykinin and thapsigargin induced Ca^{2+} entry by tyrosine kinase inhibitors. *J. Biol. Chem.* **268:**9945–9948
15. Lückhoff, A., Clapham, D.E. 1994. Calcium channels activated by depletion of internal calcium stores in A431 cells. *Biophys. J.* **67:**177–182
16. Marriott, I., Bost, K.L., Mason, M.J. 1994. The role of intracellular Ca^{2+} stores in the regulation of electrogenic plasma membrane Ca^{2+} uptake in a B-lymphocytic cell line. *J. Cell. Physiol.* **161:**441–448
17. Marriott, I., Mason, M.J. 1995. ATP depletion inhibits capacitative Ca^{2+} entry in rat thymic lymphocytes. *Am. J. Physiol.* (*in press*)
18. Mason, M.J., Grinstein, S. 1993. Ionomycin activates an electrogenic Ca^{2+} influx pathway in rat thymic lymphocytes. *Biochem. J.* **296:**33–39
19. Mason, M.J., Mahaut-Smith, M.P., Grinstein, S. 1991. The role of intracellular Ca^{2+} in the regulation of the plasma membrane Ca^{2+} permeability of unstimulated rat lymphocytes. *J. Biol. Chem.* **266:**10872–10879
20. Mason, M.J., Mayer, B., Hymel, L.J. 1993. Inhibition of Ca^{2+}

transport pathways in thymic lymphocytes by econazole, miconazole, and SKF 96365. *Am. J. Physiol.* **33:**C654–C662

21. Mason, M.J., Schofield, G.G. 1996. Ionomycin reversibly activates an inward Ca^{2+} current in rat basophilic leukemia cells (RBL-1). *Biophys. J* **70:**A322
22. McKoskey, M.A., Cahalan, M.D. 1990. G protein control of potassium channel activity in a mast cell line. *J. Gen. Physiol.* **95:**205–227
23. Ng, J., Fredholm, B.B., Jondal, M., Andersson, T. 1988. Regulation of receptor-mediated calcium influx across the plasma membrane in a human leukemic T-cell line; evidence of its dependence on an initial calcium mobilization from intracellular stores. *Biochim. Biophys. Acta* **971:**207–214
24. Ng, J., Gustavsson, J., Jondal, M., Andersson, T. 1990. Regulation of calcium influx across the plasma membrane of the human T-leukemic cell line, Jurkat: Dependence on a rise in cytosolic free calcium can be dissociated from formation of inositol phosphates. *Biochim. Biphys. Acta* **1053:**97–105
25. Pandol, S.J., Schoeffield-Payne, M.S. 1990. Cyclic GMP mediates the agonist-stimulated increase in plasma membrane calcium entry in the pancreatic acinar cells. *J. Biol. Chem.* **265:**12846–12853
26. Parekh, A.B., Penner, R. 1995. Activation of store-operated calcium influx at resting $InsP_3$ levels by sensitization of the $InsP_3$ receptor in rat basophilic leukemia cells. *J. Physiol.* **489:**377–382
27. Premack, B.A., McDonald, T.V., Gardner, P. 1994. Activation of Ca^{2+} current in Jurkat T cells following the depletion of Ca^{2+} stores by microsomal Ca^{2+}-ATPase inhibitors. *J. Immunol.* **152:**5226–5240
28. Putney, J.W. Jr., Bird, G.St.J. 1993. The inostitol phosphate-calcium signaling system in nonexcitable cell. *Endocrine Reviews* **14:**610–631
29. Randriamampita, C., Tsien, R.Y. 1993. Emptying of intracellular Ca^{2+} stores releases a novel small messenger that stimulates Ca^{2+} influx. *Nature* **364:**809–814
30. Randriamampita, C., Tsien, R.Y. 1994. Degradation of a calcium influx factor (CIF) can be blocked by phsophatase inhibitors or chelation of Ca^{2+}. *J. Biol. Chem.* **270:**29–32
31. Rossier, M.F., Bird, G. St. J., Putney, J.W. Jr. 1991. Structural organization of the ionositol 1,4,5-trisphosphate-sensitive organelle in rat liver. Evidence for linkage to the plasma membrane through actin mocro-filaments. *Biochem. J.* **274:**643–650
32. Sargeant, P., Farndale, R.W., Sage, S.O. 1993. ADP- and thapsigargin-evoked Ca^{2+} entry and protein-tyrosine phosphorylation are inhibited by the tyrosine kinase inhibitors genistein and Methyl-2,5-dihydroxycinnamate in fura-2-loaded human platelets. *J. Biol. Chem.* **268:**18151–18156
33. Sargeant, P., Farndale, R.W., Sage, S.O. 1993. The tyrosine kinase inhibitors methyl 2,5-dihydroxycinnamate and genistein reduce thrombin-evoked tyrosine phophorylation and Ca^{2+} entry in human platelets. *FEBS Lett.* **315:**242–246
34. Somasundaram, B., Mahaut-Smith, M.P. 1994. Three cation influx currents activated by purinergic receptor stimulation in rat megakaryocytes. *J. Physiol.* **480:**225–231
35. Tepel, M., Kuhnapfel, S., Theilmeier, G., Teupe, C., Scholtozmann, R., Zidek, W. 1994. Filling state of intracellular Ca^{2+} pools triggers trans plasma membrane Na^+ and Ca^{2+} influx by a tyrosine kinase-dependent pathway. *J. Biol. Chem.* **269:**26239–26242
36. Vaca, L., Kunze, D.L. 1994. Depletion of intracellular Ca^{2+} stores activates a Ca^{2+}-selective channel in vascular endothelium. *Am. J. Physiol.* **267:**C920–C925
37. von Tscharner, V., Prod'hom, B., Baggiolini, M., Reuter, H. 1986. Ion channels in human neutrophils activated by a rise in free cytosolic calcium concentration. *Nature* **324:**369–372
38. Vostal, J.G., Jackson, W.L., Shulman, N.R. 1991. Cytosolic and stored calcium antagonistically control tyrosine phosphorylation of specific platelet proteins. *J. Biol. Chem.* **266:**16911–16916
39. Wilson, O., Marriott, I., Mahaut-Smith, M.P., Hymel, L.J., Mason, M.J. 1994. Isolation and characterization of membrane potential changes associated with release of calcium from intracellular stores in rat thymic lymphocytes. *J. Membrane Biol.* **137:**159–168
40. Wischmeyer, E., Lentes, K.U., Karschin, A. 1995. Physiological and molecular characterization of an IRK-type inward rectifier K^+ channel in a tumour mast cell line. *Pfluegers Arch.* **429:**809–819
41. Worley III, J., McIntyre, M.S., Spencer, B., Duke, I.D. 1994. Depletion of intracellular Ca^{2+} stores activates a maitotoxin-sensitive nonselective cationic current in β-cells. *J. Biol. Chem.* **269:**32055–32058
42. Zhang, L., McCloskey, M.A. 1995. Immunoglobulin E receptor-activated calcium conductance in rat mast cells. *J. Physiol.* **438:**59–66
43. Zweifach, A., Lewis, R.S. 1993. Mitogen-regulated Ca^{2+} current of T-lymphocytes is activated by depletion of intracellular Ca^{2+} stores. *Proc. Nat. Acad. Sci. USA* **90:**6295–6299
44. Zweifach, A., Lewis, R.S. 1995. Rapid inactivation of depletion-activated calcium current (I_{CRAC}) due to local calcium feedback. *J. Gen. Physiol.* **105:**209–226